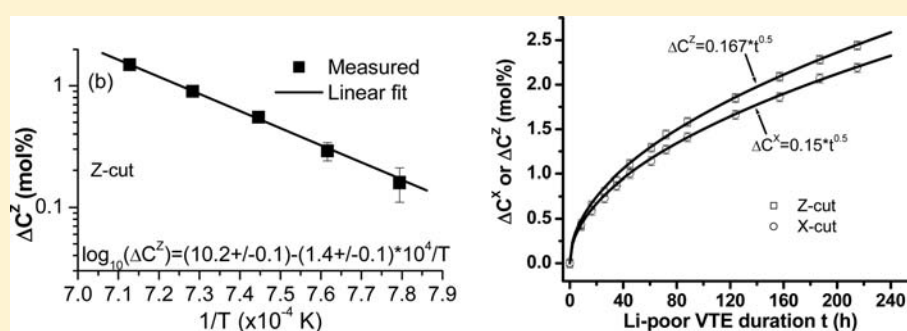


Influence of Postgrowth Li-Poor Vapor-Transport Equilibration on the Surface Li₂O Content of a Congruent LiNbO₃ Crystal

De-Long Zhang,^{*,†,‡} Bei Chen,[†] Ping-Rang Hua,^{†,‡} and Edwin Yue-Bun Pun[‡]

[†]Department of Opto-electronics and Information Engineering, School of Precision Instruments and Opto-electronics Engineering, and Key Laboratory of Optoelectronic Information Technology, Ministry of Education, Tianjin University, Tianjin 300072, People's Republic of China

[‡]Department of Electronic Engineering, City University of Hong Kong, 83 Tat Chee Avenue, Kowloon, Hong Kong, People's Republic of China



ABSTRACT: The influence of Li-poor vapor-transport equilibration (VTE) on the surface Li₂O content of initially congruent X- and Z-cut LiNbO₃ crystal plates was studied against the VTE temperature and time. The VTE-induced surface-Li₂O-content reduction was evaluated from the measured birefringence. The results show that the reduction and VTE temperature follow the traditional Arrhenius law with a surface-Li₂O-content alteration constant of $(1.0 \pm 0.2) \times 10^8 / (1.6 \pm 0.2) \times 10^{10}$ mol % and an activation energy $(2.2 \pm 0.2) / (2.8 \pm 0.2)$ eV for the X/Z-cut plate, and the reduction has a square-root dependence on the VTE time, $\Delta C^X = 0.15t^{0.5}$ for the X-cut plate and $\Delta C^Z = 0.167t^{0.5}$ for the Z-cut plate. A generalized empirical expression that relates the reduction to both the VTE temperature and duration is presented. The expression is useful for producing an off-congruent, Li-deficient LiNbO₃ plate with the desired surface Li₂O content via adjustment of the VTE temperature and duration. On the basis of the known VTE time dependence on the surface-Li₂O-content reduction, a solution to the Li⁺ out-diffusion equation, an integral of the error function complement, is obtained and verified by previously reported experimental results. The results also show that the VTE displays slight anisotropy and is slightly faster along the optical axis direction of the crystal. The Li-poor VTE is a slow process. At 1100 °C, the Li-poor VTE time required for the surface Li₂O content reaching the Li-deficient boundary is about 400/323 h for the X/Z-cut plate.

INTRODUCTION

Because of its wide transparency range and excellent electro-optical, acoustooptical, and nonlinear-optical properties, the LiNbO₃ (LN) crystal is extensively studied and called “optical silicon”. The crystal may find wide applications in the fields of electrooptics, acoustooptics, nonlinear optics, and guided-wave optics. When the [Li]/[Nb] ratio in the crystal is close to the unity, the crystal, named the near-stoichiometric (NS) LN, exhibits a number of attractive advantages over the congruent material such as stronger electrooptical¹ and nonlinear-optical effects² and largely lowered coercive field strength needed for ferroelectric domain reversal.^{3,4} Moreover, an NS LN only needs a small amount of MgO (>0.8 mol %) to prevent the photorefractive effect.^{5,6} An NS LN crystal doped with moderate MgO concentration is a more promising material for nonlinear (integrated) optics. On the other hand, an off-congruent, lithium (Li)-deficient LN crystal may find its application in the field of active waveguide devices. Over the

past years, a family of titanium (vapor zinc)-diffused erbium (Er):LN active waveguide lasers (amplifiers) and integrated devices operated in the IR regime have been demonstrated.^{7–15} For a practical Er:LN active waveguide device, selective Er³⁺ doping is a prerequisite for monolithic integration of active (optically pumped, rare-earth-doped) and passive (unpumped) devices on the same substrate, to avoid the undesired reabsorption in unpumped rare-earth-doped waveguides. Local Er³⁺ doping in an LN is usually realized via the thermal diffusion of Er metal or its oxide at a temperature close to the Curie point of the crystal (1142.3 ± 0.7 °C at the congruent point). The study on Er³⁺ diffusion into the LN crystal has shown that the solubility of Er³⁺ in the LN crystal is limited.^{16,17} In the congruent LN, the solubility is only ~1.4 mol % at the Curie point.¹⁶ Because the laser or amplifier gain depends on

Received: July 1, 2012

Published: August 16, 2012

Table 1. Summary of the Measured Birefringence (at the 1553, 1311, and 633 nm Wavelengths), Evaluated Li₂O Content, and Its Reduction at a Crystal Surface of 1-mm-Thick, Initially Congruent X- and Z-Cut LN Plates That Have Undergone the Respective Li-Poor VTE Treatment at 1010, 1040, 1070, 1100, and 1130 °C for 26 h^a

Li-poor VTE condition	cut of the plate	initial Li ₂ O content (mol %)	birefringence ($\times 10^{-2}$)			mean Li ₂ O content (mol %)	ΔC (mol %)
			1553 nm	1311 nm	633 nm		
1010 °C, 26 h	X	48.48	7.13	7.25	8.19	48.28	0.20
	Z	48.51	7.18	7.31	8.25	48.34	0.17
1040 °C, 26 h	X	48.48	6.98	7.11	8.04	48.13	0.35
	Z	48.51	7.06	7.20	8.13	48.22	0.29
1070 °C, 26 h	X	48.48	6.83	6.96	7.87	47.96	0.52
	Z	48.51	6.82	7.98	7.85	47.96	0.55
1100 °C, 26 h	X	48.48	6.58	6.71	7.59	47.68	0.80
	Z	48.51	6.52	6.65	7.52	47.61	0.90
1130 °C, 26 h	X	48.48	6.22	6.35	7.19	47.28	1.20
	Z	48.51	6.00	6.10	6.93	47.01	1.50

^aFor reference, the initial Li₂O content evaluated from the measured birefringence is also included for each sample.

the concentration of the active ions, the relatively low solubility of Er³⁺ ions in the congruent LN limits further demonstration of more efficient devices. The Er³⁺ solubility depends on not only the diffusion temperature but also the Li₂O content in the crystal. Under the same temperature, the lower the Li₂O content in the crystal is, the more the intrinsic defects present in the crystal are, the more the Er ions that can be accepted are, and hence the higher the Er³⁺ solubility would be. To increase the rare-earth-ion solubility and diffusivity, an off-congruent, Li-deficient LN is desired.

Although the LN phase exists over a wide solid solution range, roughly from 44 to 50 mol % Li₂O content, almost all commercially produced LN crystals have the congruent composition (48.4–48.6 mol % Li₂O content). Vapor-transport equilibration (VTE) is a practical method used to modify the Li₂O content of a pure or doped LN. As an alternative, an off-congruent, Li-deficient LN substrate can be prepared by carrying out a postgrowth Li-poor VTE treatment on a congruently grown crystal plate. The Li-poor VTE involves Li diffusion out of the crystal (i.e., the Li₂O vaporization via the crystal surface) and is a dynamic process. The Li₂O content at the crystal surface varies with both the VTE temperature and time. To understand the VTE process and produce an off-congruent, Li-deficient LN plate with the desired surface Li₂O content, it is crucial to have knowledge of the VTE-induced surface-Li₂O-content reduction as a function of both the VTE temperature and duration. The present work focuses on this aspect of study.

EXPERIMENTAL DESCRIPTION

Six X-cut and six Z-cut commercially congruent LN plates with optical-grade surfaces were used for the present study. These plates, having a typical thickness of 1 mm, were annealed in a Li-poor atmosphere created by a sealed niobium (Nb)-rich two-phase crucible at elevated temperature. A Li-poor technique similar to that reported by Bordui et al.¹⁸ was employed in this work. The two-phase crucible was prepared by sintering the homogeneous mixture of Li₂CO₃ and Nb₂O₅ powder, which have the same purity of 99.99%. The molar ratio of Li₂CO₃ and Nb₂O₅ was 40:60 (mol %) in the Nb-rich mixture. The mixture was pressurized and molded into a crucible model of 6 cm inner diameter and 4 cm height. A precalcination at 1000 °C for 10 h and an additional calcination at 1100 °C for 1 h produced an Nb-rich two-phase crucible. The solid-phase chemical reaction involved is 40 mol % Li₂CO₃ + 60 mol % Nb₂O₅ = 40 mol % CO₂↑ + 60 mol % LiNbO₃ + 20 mol % LiNb₃O₈. Congruent crystal plates to be treated were wrapped with platinum wires to avoid contact with the two-phase

powder, which was contained in the two-phase crucible prior to the crystal plates to be treated. Then, the crucible was sealed with a lid, which was made of the two-phase powder also. Subsequently, the crucible was heated up to the target temperature and dwelled for the scheduled duration. Because of the Li concentration gradient inside and outside the crystal, the Li ions in the bulk of the crystal diffuse out of the crystal surface at elevated temperature and the crystal releases Li₂O gas, which sinks in the Nb-rich two-phase powder because of the solid-phase reaction Li₂O↑ + LiNb₃O₈ = 3LiNbO₃. As a result, the original congruent crystal becomes more and more Li-deficient because of continuous Li₂O loss from the crystal.

At first, the samples used for the study of the VTE temperature dependence of the surface-Li₂O-content reduction were prepared. A total of 10 of the 12 LN plates were selected and independently subjected to five VTE cycles in total. In each cycle, a pair of X- and Z-cut plates was treated. The VTE duration was fixed at 26 h, while the temperature was varied from 1010 to 1040, 1070, 1100, and 1130 °C. Table 1 summarizes the VTE conditions of the five cycles. After each VTE cycle, the Li₂O-content reduction on the crystal surface was indirectly determined by measurement of the birefringence at the wavelengths of 633, 1311, and 1553 nm.

The remaining two LN plates were used for the study of the VTE time dependence on the surface-Li₂O-content reduction. Both plates were consecutively subjected to a series of Li-poor VTE cycles. The VTE temperature was fixed at 1100 °C. The duration varied from 0 to 220 h in a step from a few hours to several tens of hours. After each VTE cycle, the Li₂O-content reduction on the crystal surface was also determined by measurement of the birefringence.

Measurement of the birefringence (i.e., measurement on the ordinary and extraordinary refractive indices) was accomplished by a Metricon 2010 prism coupler (Metricon Corp., Pennington, NJ), which has a working principle of measurement on the critical angle of total reflection. Note that the refractive index measured by this method should be the value at the crystal surface because the total reflection phenomenon takes place there. It is convenient to choose a transverse-magnetic or -electric polarization scheme to measure the ordinary or extraordinary index, depending on the cut of the plate to be measured. All of the measurements were carried out at room temperature (24.5 ± 0.1 °C).

RESULTS AND DISCUSSION

The Li composition in an LN crystal can be determined by many optical and nonoptical methods.¹⁹ Here, the optical method of the birefringence measurement was used to quantitatively evaluate the Li₂O content at the surface of the studied samples. Schlarb and Betzler have established a Li₂O-content-dependent Sellmeier equation.²⁰ By utilizing this equation, one can evaluate the Li₂O content from the measured

birefringence. The evaluations at the wavelengths 633, 1311, and 1553 nm give an averaged result of the Li_2O content. The measurement error of the refractive index, $\pm 5 \times 10^{-4}$, yields a Li_2O -content uncertainty of ± 0.05 mol %. For reference purposes, the birefringence measurement was also carried out on the congruent plate before the VTE treatment and the Li_2O content was evaluated in a similar way. Table 1 brings together the evaluated Li_2O contents of all of the initial congruent plates. One can see that all of the initial congruent LN plates have the same Li_2O content of 48.60 ± 0.05 mol %, consistent with the nominal value of 48.4–48.6 mol %. The consistency implies that the Li_2O -content data evaluated from the birefringence measurement are convincing.

A. VTE Temperature Dependence of the Surface Li_2O Content. Table 1 summarizes the measured birefringence at the 1553, 1311, and 633 nm wavelengths, the evaluated mean Li_2O content, and the reduction of ΔC (relative to the initial Li_2O -content value) at the surface of the LN plates that had undergone VTE treatments under the five different temperatures of 1010, 1040, 1070, 1100, and 1130 °C. For the X-cut plates, the VTE-induced surface- Li_2O -content reduction ΔC is 0.20, 0.35, 0.52, 0.80, and 1.20 ± 0.05 mol % for VTE temperatures of 1010, 1040, 1070, 1100, and 1130 °C, respectively. For the Z-cut plates, the reduction is 0.17, 0.29, 0.55, 0.90, and 1.50 ± 0.05 mol % in order. These surface ΔC values indicate that the Li-poor VTE at the crystal surface has a slight plate-cut effect at higher temperature. It is slightly faster on the surface of the Z-cut plate. As expected, the ΔC value increases with a rise in the VTE temperature. To further quantify the temperature dependence, the ΔC value is plotted against the inverse VTE temperature $1/T$ on a semilogarithmic scale in Figure 1 (see the full circles in part a for the X-cut plates and the full squares in part b for the Z-cut plates). The experimental error is indicated for each data.

It is found that ΔC^i ($i = X$ or Z) and VTE temperature T are well related by the traditional Arrhenius law, given by

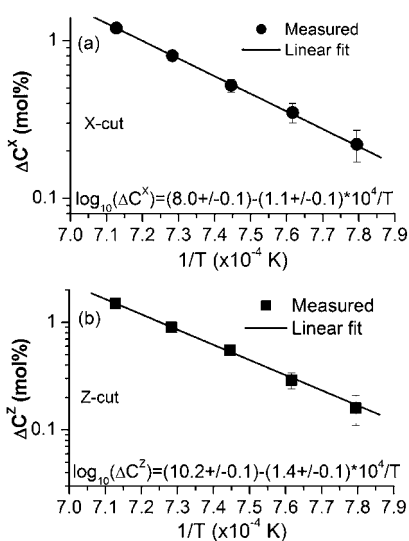


Figure 1. 26 h Li-poor VTE-induced surface- Li_2O -content reduction ΔC (full circles or squares) versus $1/T$ on a semilogarithmic scale for initially congruent (a) X-cut and (b) Z-cut LN plates. The solid line represents the linear fit to the full circles in part a and full squares in part b. The fitting expression is indicated for each case.

$$\Delta C^i(T) = \Delta C_0^i \exp\left(-\frac{E_a^i}{k_B T}\right) \quad (1)$$

where k_B is the Boltzmann constant, ΔC_0^i ($i = X$ or Z) is the surface- Li_2O -content alteration constant, and E_a^i ($i = X$ or Z) is the activation energy for the X- or Z-cut plate. The solid-line curves in Figure 1 represent the linear fits to the experimental data on the semilogarithmic scale. The fitting expression is indicated for each case. It is $\log_{10}(\Delta C^X) = (8.0 \pm 0.1) - (1.1 \pm 0.1) \times 10^4/T$ for the X-cut plates and $\log_{10}(\Delta C^Z) = (10.2 \pm 0.1) - (1.4 \pm 0.1) \times 10^4/T$ for the Z-cut plates. By correlating the two fitting expressions with eq 1, one can find the surface- Li_2O -content alteration constant ΔC_0^i and the activation energy E_a^i . They are respectively $(1.0 \pm 0.2) \times 10^8$ mol % and 2.2 ± 0.2 eV for the X-cut plates and $(1.6 \pm 0.2) \times 10^{10}$ mol % and 2.8 ± 0.2 eV for the Z-cut plates.

B. VTE Duration Dependence of the Surface Li_2O Content. Figure 2 shows the VTE (at 1100 °C)-induced

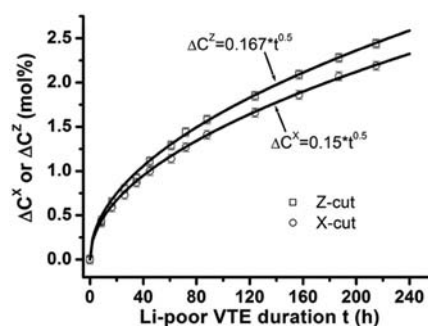


Figure 2. Li-poor VTE duration dependence on the VTE (at 1100 °C)-induced Li_2O -content reduction on the surface of 1-mm-thick, initially congruent X-cut (open circles) and Z-cut (open squares) LN plates. The error is given for each open circle/square data. The solid-line curves represent the best square-root fits to the scattered data. The fitting expressions are indicated.

surface- Li_2O -content reduction ΔC against the VTE duration t . The open circles show the reduction on the surface of the X-cut plate, and the open squares show the case of the Z-cut plate. It is expected that the surface- Li_2O -content reduction increases with an increase in the VTE duration for both cases of X- and Z-cut plates. Both measured plots can be well fitted by a square-root dependence on the VTE duration t . The solid-line curves in Figure 2 denote the fitting results. The fitting expression is $\Delta C^X(t) = 0.15t^{0.5}$ for the X-cut plate and $\Delta C^Z(t) = 0.167t^{0.5}$ for the Z-cut plate. The two expressions reveal that VTE shows a slight plate-cut effect and is slightly faster on the surface of the Z-cut plate. This conclusion is consistent with that deduced from the above-mentioned results of ΔC^i against the VTE temperature. Very different from the Li-rich VTE case, the Li-poor VTE requires a much longer time for the surface Li_2O content to reach the Li-deficient boundary, where the Li_2O -content reduction ΔC is predicted to be ~ 3 mol % at 1100 °C according to the $\text{Li}_2\text{O}-\text{Nb}_2\text{O}_5$ phase diagram.¹⁸ The time required is around 400 h for the X-cut plate and 323 h for the Z-cut plate. Instead, for the case of the Li-rich VTE, the time required to reach the Li-rich boundary (i.e., the stoichiometric composition) is only around 20 h.²¹ It is thus concluded that the Li-poor VTE process is much slower than the Li-rich VTE process, consistent with the previously reported result.¹⁸ It should be stressed that the empirical expressions given above

are only valid for the case that the surface Li₂O content does not reach the Li-deficient boundary. As long as the Li-poor VTE duration is longer than 400 h for the X-cut plate and 323 h for the Z-cut plate, the two empirical expressions are no longer valid.

With the known VTE duration dependence of the surface-Li₂O-content reduction, it is possible to solve the mathematical model valid for the Li-poor VTE process. Here we consider a one-dimensional Cartesian reference frame fixed at the top surface of the crystal with the x (z) axis pointing to the depth direction of the X (Z)-cut plate. According to the diffusion theory, the one-dimensional Li⁺ out-diffusion process here is described by a standard Fick-type diffusion equation with a Li₂O-content-dependent diffusion coefficient, given by

$$\frac{\partial \Delta C^X(x, t)}{\partial t} = \frac{\partial}{\partial x} \left\{ D^X[\Delta C^X(x, t)] \frac{\partial \Delta C^X(x, t)}{\partial x} \right\}$$

for X-cut plates (2)

$$\frac{\partial \Delta C^Z(z, t)}{\partial t} = \frac{\partial}{\partial z} \left\{ D^Z[\Delta C^Z(z, t)] \frac{\partial \Delta C^Z(z, t)}{\partial z} \right\}$$

for Z-cut plates (3)

where $\Delta C^X(x, t)$ or $\Delta C^Z(z, t)$ denotes the Li₂O-content reduction at the depth position x or z after a given diffusion time t , and $D^X[\Delta C^X(x, t)]$ and $D^Z[\Delta C^Z(z, t)]$ are the Li⁺ diffusivities, which are dependent on the Li₂O content.

When the Li₂O-content reduction at the boundary $\Delta C^X(x=0, t)$ or $\Delta C^Z(z=0, t)$ has a square-root dependence on the diffusion time t , like the case of the diffusion system studied here, the solution to eqs 2 and 3 is an integral of error function complement (ierfc),²² given by

$$\Delta C^X(x, t) = 2J\sqrt{t/D^X[\Delta C^X(x, t)]} \text{ierfc}\{x / [2\sqrt{D^X[\Delta C^X(x, t)]t}]\}$$

for X-cut plates (4)

$$\Delta C^Z(z, t) = 2J\sqrt{t/D^Z[\Delta C^Z(z, t)]} \text{ierfc}\{z / [2\sqrt{D^Z[\Delta C^Z(z, t)]t}]\}$$

for Z-cut plates (5)

where J is the mass-transport flux at the crystal surface and is determined by the Li₂O-content gradient at the surface

$$J = D^X[\Delta C^X(0, t)] \left[\frac{\partial \Delta C^X(x, t)}{\partial x} \right]_{x=0}$$

for X-cut plates (6)

$$J = D^Z[\Delta C^Z(0, t)] \left[\frac{\partial \Delta C^Z(z, t)}{\partial z} \right]_{z=0}$$

for Z-cut plates (7)

The surface-Li₂O-content alteration can be determined from eqs 4 and 5 as

$$\Delta C^X(0, t) = 2\{J/\sqrt{D^X[\Delta C^X(0, t)]}\}\sqrt{t/\pi}$$

for X-cut plates (8)

$$\Delta C^Z(0, t) = 2\{J/\sqrt{D^Z[\Delta C^Z(0, t)]}\}\sqrt{t/\pi}$$

for Z-cut plates (9)

which, as expected, show a square-root dependence on the diffusion time t . It is worthwhile to note that the ierfc solutions (4) and (5) are verified by the previous experimental results.²³

C. Dependence of the Surface-Li₂O-Content Reduction on Both the VTE Temperature and Duration. In combination with the above-mentioned empirical relationship of the surface-Li₂O-content reduction ΔC to the VTE temperature T , a unified expression for $\Delta C(T, t)$ can be written as

$$\Delta C^i(T, t) = \alpha^i \Delta C_0^i \exp\left(-\frac{E_a^i}{k_B T}\right) \sqrt{t}$$

(10)

where the coefficient $\alpha^X = 0.19$ for the X-cut plate and $\alpha^Z = 0.17$ for the Z-cut plate. As mentioned above, the empirical expression (10) is only valid for the case that the surface Li₂O content does not exceed the Li-deficient boundary. For example, at 1100 °C, ΔC is around 3 mol % at the Li-deficient boundary. As long as the VTE duration is longer than 400 h for the X-cut plate and 323 h for the Z-cut plate, the VTE reaches equilibrium, the surface Li₂O content remains a constant composition, and the empirical expression is no longer valid. By utilizing eq 10, one can design the VTE temperature and duration for the desired surface Li₂O content.

Finally, it should be pointed out that some problems may exist as an off-congruent, Li-deficient LN is applied to develop an active waveguide device. First, as we know, the Curie temperature (T_c) of the LN crystal (1142.3 ± 0.7 °C at the congruent point) is closely related to the Li₂O content inside the crystal, $C(\text{Li}_2\text{O})$, and both follow the linear relationship $T_c = 39.064 C(\text{Li}_2\text{O}) - 746.73$.¹⁸ This implies that the ferroelectric domain in a Li-deficient crystal orients no longer conformably but randomly. Second, as the crystal composition decreases, the electrooptical effect of the crystal degrades.¹ These two problems would be solved by carrying out further Li compensation (via the Li-rich VTE process) at first and then the uniform ferroelectric poling treatment on the whole crystal plate after the rare-earth-doping and subsequent waveguide fabrication procedures. In addition, the high Er³⁺-doping concentration inevitably results in increases of the clustering Er³⁺ site concentration, the cooperative upconversion probability, which depends mainly on the clustering site concentration, and the concentration quenching effect on the 1.5 μm fluorescence intensity, which is associated with the upconversion effect. It is anticipated that there should be a trade-off between the Er³⁺ concentration and the concentration quenching effect. All of these are intended to be in the future work.

CONCLUSIONS

Now we have gained complete knowledge about the Li-poor VTE treatment of an LN plate. The present study allows us to conclude the following five points: (1) The VTE-induced surface-Li₂O-content reduction and the VTE temperature follow the traditional Arrhenius law with a surface-Li₂O-content alteration constant $(1.0 \pm 0.2) \times 10^8 / (1.6 \pm 0.2) \times 10^{10}$ mol % and an activation energy $(2.2 \pm 0.2) / (2.8 \pm 0.2)$ eV for the X/Z-cut plate. (2) The VTE-induced surface-Li₂O-content reduction has a square-root dependence on the VTE duration, $\Delta C^X(t) = 0.15t^{0.5}$ for the X-cut plate and $\Delta C^Z(t) = 0.167t^{0.5}$ for the Z-cut plate. (3) A generalized expression that relates the VTE-induced surface-Li₂O-content reduction to both the VTE temperature and duration is presented. By using this empirical

expression, one can design the VTE temperature and duration needed for producing an off-congruent, Li-deficient LN plate with the desired surface Li_2O content. (4) The VTE shows slight anisotropy and is slightly faster along the z (optical axis of crystal) direction. The Li-poor VTE process is much slower than the Li-rich VTE process. At 1100 °C, the Li-poor VTE time required for the surface Li_2O content to reach the Li-deficient boundary is about 400/323 h for the X/Z-cut plate. (5) The Li-poor VTE process (i.e., the Li^+ out-diffusion process) follows the standard one-dimensional Fick-type diffusion equation with a Li_2O -content-dependent diffusion coefficient. The equation has a solution of an *ierfc*.

In addition, the previous studies revealed that the Li^+ diffusivity is Li_2O -content-dependent.²¹ The diffusivity at 1100 °C has a value of $0.4 \mu\text{m}^2/\text{s}$ at the congruent point. It decreases with decreasing Li_2O content, and the decrease is by at least one order of magnitude as the Li_2O content decreases by 1 mol % from the congruent point. Moreover, for a given Li_2O content, the Li^+ diffusivity is nearly doubled as the diffusion temperature is increased from 1100 to 1130 °C.²³

AUTHOR INFORMATION

Corresponding Author

*E-mail: dlzhang@tju.edu.cn.

Notes

The authors declare no competing financial interest.

ACKNOWLEDGMENTS

This work was supported by the National Natural Science Foundation of China under Projects 50872089 and 61077039 by the Key Program for Research on Fundamental to Application and Leading Technology, by the Tianjin Science and Technology Commission of China under Project 11JCZDJC15500, and by Specialized Research Fund for the Doctoral Program of Higher Education of China under Project 20100032110052.

REFERENCES

- (1) Fujiwara, T.; Takahashi, M.; Ohama, M.; Ikushima, A. J.; Furukawa, Y.; Kitamura, K. *Electron. Lett.* **1999**, *35*, 499–501.
- (2) Fujiwara, T.; Ikushima, A. J.; Furukawa, Y.; Kitamura, K. *Technical Digest of Meeting on New Aspects of Nonlinear Optical Materials and Devices*; Institute for Molecular Science, IEEE: Okazaki, Japan, 1999; pp 2–4.
- (3) Gopalan, V.; Mitchell, T. E.; Furukawa, Y.; Kitamura, K. *Appl. Phys. Lett.* **1998**, *72*, 1981–1983.
- (4) Grisard, A.; Lallier, E.; Polgar, K.; Peter, A. *Electron. Lett.* **2000**, *36*, 1043–1044.
- (5) Péter, Á.; Polgár, K.; Kovács, L.; Lengyel, K. *J. Cryst. Growth* **2005**, *284*, 149–155.
- (6) Furukawa, Y.; Kitamura, K.; Takekawa, S.; Miyamoto, A.; Terao, M.; Suda, N. *Appl. Phys. Lett.* **2000**, *77*, 2494–2496.
- (7) Becker, Ch.; Oesselke, T.; Pandavenes, J.; Ricken, R.; Rochhausen, K.; Schreiber, G.; Sohler, W.; Suche, H.; Wessel, R.; Balsamo, S.; Montrosset, I.; Sciancalepore, D. *IEEE J. Sel. Top. Quantum Electron.* **2000**, *6*, 101–113.
- (8) Amin, J.; Aust, J. A.; Sanford, N. A. *Appl. Phys. Lett.* **1996**, *69*, 3785–3787.
- (9) Helmfriid, S.; Arvidsson, G.; Webjorn, J.; Linnarsson, M.; Pihl, T. *Electron. Lett.* **1991**, *27*, 913–914.
- (10) Huang, C. H.; McCaughan, L. *IEEE J. Sel. Top. Quantum Electron.* **1996**, *2*, 367–372.
- (11) Huang, C. H.; McCaughan, L. *Electron. Lett.* **1997**, *33*, 1639–1640.

(12) Cantelar, E.; Torchia, G. A.; Sanz-García, J. A.; Pernas, P. L.; Lifante, G.; Cussó, F. *Appl. Phys. Lett.* **2003**, *83*, 2991–2993.

(13) Das, B. K.; Ricken, R.; Sohler, W. *Appl. Phys. Lett.* **2003**, *83*, 1515–1517.

(14) Das, B. K.; Ricken, R.; Quiring, V.; Suche, H.; Sohler, W. *Opt. Lett.* **2004**, *29*, 165–167.

(15) Schreiber, G.; Hofmann, D.; Grundkotter, W.; Lee, Y. L.; Suche, H.; Quiring, V.; Ricken, R.; Sohler, W. *Proc. SPIE* **2001**, *4277*, 144–160.

(16) Baumann, I.; Brinkmann, R.; Dinand, M.; Sohler, W.; Beckers, L.; Buchal, Ch.; Fleuster, M.; Holzbrecher, H.; Paulus, H.; Müller, K.-H.; Gog, Th.; Materlik, G.; Witte, O.; Stolz, H.; von der Osten, W. *Appl. Phys. A: Mater. Sci. Process.* **1997**, *64*, 33–44.

(17) Caccavale, F.; Segato, F.; Mansour, I.; Almeida, J. M.; Leite, A. P. *J. Mater. Res.* **1998**, *13*, 1672–1678.

(18) Bordui, P. F.; Norwood, R. G.; Jundt, D. H.; Fejer, M. M. *J. Appl. Phys.* **1992**, *71*, 875–879.

(19) Wöhlecke, M.; Corradi, G.; Betzler, K. *Appl. Phys. B: Lasers Opt.* **1996**, *63*, 323–330.

(20) Schlarb, U.; Betzler, K. *Phys. Rev. B* **1993**, *48*, 15613–15620.

(21) Jundt, D. H.; Fejer, M. M.; Norwood, R. G.; Bordui, P. F. *J. Appl. Phys.* **1992**, *72*, 3468–3473.

(22) Crank, J. *The mathematics of diffusion*, 2nd ed.; Clarendon Press: Oxford, England, 1975; p 34.

(23) Chen, B.; Hua, P. R.; Zhang, D. L.; Pun, E. Y. B. *J. Am. Ceram. Soc.* **2012**, *95*, 1018–1022.